

# UC Davis

## UC Davis Previously Published Works

### Title

Alteration of glycosphingolipid metabolism by ozone is associated with exacerbation of allergic asthma characteristics in mice

### Permalink

<https://escholarship.org/uc/item/7gt9z0db>

### Journal

Toxicological Sciences, 191(1)

### ISSN

1096-6080

### Authors

Stevens, Nathaniel C

Brown, Veneese J

Domanico, Morgan C

et al.

### Publication Date




2023-01-31

### DOI

10.1093/toxsci/kfac117

Peer reviewed

# Alteration of glycosphingolipid metabolism by ozone is associated with exacerbation of allergic asthma characteristics in mice

Nathaniel C. Stevens <sup>1</sup>, Veneese J. Brown,<sup>2</sup> Morgan C. Domanico,<sup>2</sup> Patricia C. Edwards,<sup>2</sup> Laura S. Van Winkle <sup>2,3</sup>, Oliver Fiehn <sup>1,\*</sup>

<sup>1</sup>Genome Center, University of California Davis, Davis, California 95616, USA

<sup>2</sup>Center for Health and the Environment, School of Veterinary Medicine, University of California Davis, Davis, California 95616, USA

<sup>3</sup>Department of Anatomy, Physiology and Cell Biology, School of Veterinary Medicine, University of California Davis, Davis, California 95616, USA

\*To whom correspondence should be addressed at West Coast Metabolomics Center, UC Davis Genome Center, Room 1313, 451 Health Sciences Drive, University of California Davis, Davis, CA 95616, USA. E-mail: ofiehn@ucdavis.edu.

## Abstract

Asthma is a common chronic respiratory disease exacerbated by multiple environmental factors. Acute ozone exposure has previously been implicated in airway inflammation, airway hyperreactivity, and other characteristics of asthma, which may be attributable to altered sphingolipid metabolism. This study tested the hypothesis that acute ozone exposure alters sphingolipid metabolism within the lung, which contributes to exacerbations in characteristics of asthma in allergen-sensitized mice. Adult male and female BALB/c mice were sensitized intranasally to house dust mite (HDM) allergen on days 1, 3, and 5 and challenged on days 12–14. Mice were exposed to ozone following each HDM challenge for 6h/day. Bronchoalveolar lavage, lung lobes, and microdissected lung airways were collected for metabolomics analysis ( $N=8/\text{sex}/\text{group}$ ). Another subset of mice underwent methacholine challenge using a forced oscillation technique to measure airway resistance ( $N=6/\text{sex}/\text{group}$ ). Combined HDM and ozone exposure in male mice synergistically increased airway hyperreactivity that was not observed in females and was accompanied by increased airway inflammation and eosinophilia relative to control mice. Importantly, glycosphingolipids were significantly increased following combined HDM and ozone exposure relative to controls in both male and female airways, which was also associated with both airway resistance and eosinophilia. However, 15 glycosphingolipid species were increased in females compared with only 6 in males, which was concomitant with significant associations between glycosphingolipids and airway resistance that ranged from  $R^2 = 0.33\text{--}0.51$  for females and  $R^2 = 0.20\text{--}0.34$  in male mice. These observed sex differences demonstrate that glycosphingolipids potentially serve to mitigate exacerbations in characteristics of allergic asthma.

**Keywords:** ozone; metabolomics; sphingolipids; LC-MS/MS.

Asthma is a common chronic respiratory disease characterized by reversible airway obstruction, which is initiated by airway hyperresponsiveness (AHR), airway inflammation, and excessive mucous production. Ozone is a well-known risk factor for exacerbations in existing cases of asthma, which poses a significant public health concern to more than 123 million people in the United States that live in areas with unhealthy levels of ozone as of 2021 (American Lung Association, 2021; Guarneri and Balmes, 2014; Tetreault et al., 2016). Ozone is a potent oxidant produced by degradation of nitrogen dioxide and volatile organic compounds emitted from fossil fuel combustion by sunlight and is the primary component of photochemical smog (Mustafa, 1990). Importantly, ozone exposure elicits concentration- and time-dependent adverse effects *in vivo*, which primarily affect the major conducting airways (Bao et al., 2018; Hu et al., 1994; Rosenquist et al., 2020). Acute ozone exposure induces AHR, airway inflammation, cell apoptosis, and damages lung surfactant, whereas chronic, episodic exposure can also alter lung development and cause remodeling of the airways (Bao et al., 2017; Herring et al., 2015; Murphy et al., 2014; Williams et al., 2008).

Although some studies have implicated signaling mediators such as p38 MAPK and interleukin-17 in modulation of AHR and airway inflammation, the molecular mechanisms underlying these effects are not as well understood (Bao et al., 2017; Zhang et al., 2019a).

Sphingolipids are emerging as integral modulators of many hallmarks of asthma, including airway inflammation, immune cell infiltration, and AHR (Ammit et al., 2001; Gendron et al., 2017; Park and Im, 2019; Patil et al., 2019). Previous studies of individual sphingolipids including sphingosine 1-phosphate and expression of genes including orosomucoid-like 3 (ORMDL3) have established the role of sphingolipids in regulating processes such as mast cell degranulation, airway smooth muscle function, and ceramide synthesis that promote characteristics of asthma (Oyeniran et al., 2015; Patil et al., 2019; Price et al., 2013). Sphingolipids are synthesized from breakdown of sphingomyelin in the outer leaflet of the cell membrane as well as through *de novo* synthesis by serine palmitoyltransferase (Zhang et al., 2019b). Importantly, the breakdown of membrane-bound sphingomyelin is catalyzed by acid sphingomyelinase, which is activated by cellular injury and

results in the formation of ceramide (Böll *et al.*, 2020; Sopel *et al.*, 2019; Zeidan *et al.*, 2008). Consequently, oxidative stress and airway epithelial cell death caused by ozone exposure suggests that ozone-induced asthma exacerbations may be influenced by increased breakdown of sphingomyelin and downstream sphingolipid signaling (Mustafa, 1990). Nontargeted metabolomics assays sampling plasma and bronchoalveolar lavage fluid (BALF) from mice and humans have demonstrated perturbations in sphingolipid metabolism following ozone exposure. These findings are consistent with studies detailing the effects of ozone on surfactant and membrane lipids (Cheng *et al.*, 2018; Kim *et al.*, 2010; Miller *et al.*, 2016; Uhlson *et al.*, 2002). Despite these results, the effects of ozone exposure on sphingolipids that may contribute to asthma exacerbation have not been identified.

The objective of this study was to investigate the effects of acute ozone exposure on sphingolipid metabolism using a mouse model of allergic asthma. Male and female BALB/c mice were sensitized to house dust mite (HDM) allergen and subsequently challenged with HDM, which was followed by acute, whole-body ozone exposure. We characterized global metabolite profiles in microdissected lung airway tissue using liquid chromatography-high-resolution mass spectrometry (LC-MS/MS)-based metabolomics assays, which enabled us to connect changes in sphingolipids to perturbations in other functionally important metabolite classes. We have previously highlighted the importance of discerning site-specific metabolomic changes using microdissected lung extracts following target-specific toxicant exposure (Stevens *et al.*, 2021). Furthermore, we conducted pulmonary function testing, histological analysis, and cell differential counts in BALF to relate perturbations in sphingolipid metabolism to morphological and physiological changes following exposure. We hypothesized that sphingomyelins, ceramides, and other sphingolipid subclasses are significantly altered in response to ozone exposure, which contributes to increased airway hyperreactivity, airway inflammation, and immune cell influx in HDM-sensitized mice.

## Materials and methods

### Animal protocol

Adult male and female BALB/c mice (Envigo, Inc.) 8–10 weeks of age were acclimatized for 1 week in rooms kept on a 12/12 light/dark cycle and fed Purina 5001 lab diet. Mice were sensitized to crushed whole bodies of *Dermatophagoides farinae* (Stallergenes Greer, Inc.) dissolved in phosphate-buffered saline (PBS), challenged with HDM, and acutely exposed to ozone (Figure 1). The

sensitization phase consisted of 3 intranasal instillations of 10  $\mu\text{g}$  HDM in 25  $\mu\text{l}$  PBS or vehicle on days 1, 3, and 5 followed by 3 consecutive challenges with HDM (10  $\mu\text{g}$  in 25  $\mu\text{l}$  PBS) on days 12–14 (Castaneda and Pinkerton, 2016). Following each HDM challenge, mice were exposed to either filtered air (FA) or ozone (0.5 ppm, 6 h/day). Exposure chambers were individually monitored every hour by a Teledyne Model 400E ozone analyzer to ensure stability of ozone concentrations for the entire duration of exposure. Separate subsets of mice were used for pulmonary function testing ( $N=6$  males and 6 females/group; total  $N=48$ ) and for sample collection ( $N=8$  males and 8 females/group; total  $N=64$ ), both of which were completed 24 h after the final ozone exposure. One subset of mice was euthanized with a lethal injection of pentobarbital and necropsied to collect left lung lobes for histological staining, BALF, and right lung lobes for metabolomics analysis. Animal exposures and experiments were conducted following approved protocols reviewed by the UC Davis Institutional Animal Care and Use Committee in accordance with guidelines for animal research established by the National Institutes of Health.

### Lipidomics and polar metabolite analysis

Right lung lobes were microdissected following a previous protocol, and isolated lung airways were analyzed by our previous LC-MS/MS method, which characterized metabolomic responses to target-specific toxicants in major lung regions (Plopper *et al.*, 1991; Stevens *et al.*, 2021). These findings were further supported by our pilot data using principal components analysis (PCA) to distinguish metabolomic differences between microdissected lung regions and whole lung homogenates (Supplementary Figure 1). Briefly, gross dissected lung airways were lyophilized, and lipids and polar metabolites were extracted using a mixture of 225  $\mu\text{l}$  methanol and 750  $\mu\text{l}$  methyl *tert*-butyl ether with internal standards used in lipidomics analysis, listed in Supplementary Table 1 (Cajka and Fiehn, 2016). The resulting top and bottom fractions were evaporated to dryness, and internal standards used in polar metabolite analysis were added upon resuspension of the dried bottom sample fraction (Supplementary Table 1). All samples were analyzed by a Thermo Fisher Scientific Vanquish UHPLC + liquid chromatography system coupled to a Q-Exactive HF orbital ion trap mass spectrometer. Iterative exclusion lists were generated from repeated acquisition of pooled experimental samples to increase MS/MS coverage of low abundance metabolites within each sample

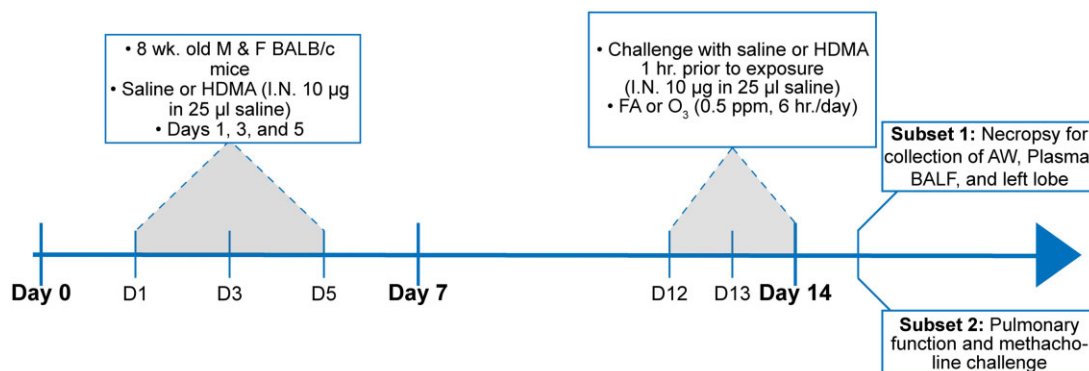


**Figure 1.** Experimental design including the protocol used for allergic sensitization and ozone exposure. One subset of mice underwent pulmonary function testing and methacholine challenge, and gross dissected airways (AW), BALF, and left lung lobes were collected from another subset of mice for downstream metabolomics, cell count, and histological analysis.

(Koelmel et al., 2017). LC and MS/MS parameters were used as given in Stevens et al. (2021).

### BALF cell counts

BALF was collected by tying off the left lobe and flushing the right lobes with 0.5 ml PBS (3×, 1.5 ml total collection volume). Samples were centrifuged and the pellet was resuspended in 0.5 ml PBS and mixed with 10 μl of Trypan Blue to perform total cell counts using a hemacytometer. The remaining resuspension volume was centrifuged using cytospin funnels onto glass slides and stained with hematoxylin and eosin (H&E). The number of macrophages, lymphocytes, neutrophils, and eosinophils was determined by calculating the proportion of each cell type per 500 cells and individual counts based on the total number of cells in each sample.

### Assessment of pulmonary function

Mice were deeply anesthetized with an intraperitoneal injection of a 0.01-ml/g solution containing 5 mg/ml telazol and 0.07 mg/ml dexdormitor 24 h after the final ozone exposure. Each mouse was connected to a mechanical ventilator (flexiVent FX2, Scireq) by inserting a cannula into the trachea. Additionally, mice received an intramuscular injection of 1 mg succinylcholine prior to initiating forced oscillations. Mice were challenged with increasing doses of methacholine (0.25, 0.5, 1, 2, 4, and 8 mg/ml), and the ventilation frequency and tidal volume for each mouse were set at 150 breaths/min and 10 ml/kg, respectively. A forced oscillation maneuver performed at the ventilation rate of each animal enabled measurements of whole respiratory system resistance, elastance, and compliance. Additional forced oscillation perturbations above and below the ventilation frequency measured respiratory impedance, which was used to quantify airway resistance using a constant-phase model. If the procedure lasted longer than 20 min, mice were injected with half of the original dose of anesthesia to prevent premature recovery. Mice were continuously monitored and were euthanized with a lethal injection of pentobarbital following methacholine challenge.

### Lung histology

Left lung lobes were fixed with 1% paraformaldehyde in PBS for 24 h and promptly transferred to 70% ethanol. The storage time in ethanol ranged from 6 to 8 weeks prior to embedding in paraffin. Paraffin sections 5 μm thick were deparaffinized, stained with H&E or alcian blue/Periodic acid-Schiff (AB/PAS) stain, and subsequently imaged using an Olympus BH-2 microscope with a 10× objective. Representative images were selected to assess inflammation, thickening, and narrowing of proximal airways within each treatment group (N = 3 males and 3 females/group; total N = 24).

### Data processing and statistical analysis

Metabolomics data processing was completed using MS-DIAL v.4.70 (Tsugawa et al., 2015). Compound identification was based on accurate mass, retention time, and MS/MS matches to spectra in MassBank of North America (<https://massbank.us>, last accessed November 08, 2022), NIST 20, and *in silico* libraries (Bonini et al., 2020). Samples were normalized to the total ion chromatogram of all annotated metabolites and log transformed. Statistical analysis was completed in R v.4.1.1, and 1-way ANOVA with Tukey's HSD *post hoc* analysis was performed to determine statistical significance unless otherwise noted. PCA, an unsupervised multivariate data reduction technique, was used to distinguish global changes in metabolite profiles within each sample.

Chemical similarity enrichment analysis (ChemRICH) subsequently determined statistically significant differences in structurally related metabolites (Barupal and Fiehn, 2017).

## Results

### Metabolomics annotations and technical variance

Lipidomics and polar metabolite analysis yielded 820 unique metabolites across both positive and negative ionization modes, including 73 sphingolipids and precursors involved in sphingolipid synthesis (Supplementary Tables 2 and 3). Unknown metabolites were excluded from statistical analysis, and the full metabolite list with annotation criteria and normalized peak heights is provided in Supplementary File 1. Neutral and polar lipids such as triacylglycerides, phosphatidylcholines (PC), and phosphatidylethanolamines (PE) constituted about half of the total number of lipids identified. Additionally, 31 sphingomyelins, 19 ceramides, and 12 hexosylceramides as well as 12 oxidized species derived from each of these subclasses were annotated. Technical variance was also assessed prior to statistical analysis for all analytical platforms. The median values for relative standard deviation among identified metabolites in pooled experimental samples were 6% and 26.1% for lipidomics and polar metabolite analysis, respectively.

### Combined HDM and ozone exposure significantly alters airway sphingolipids compared with controls

We first characterized the effects of ozone exposure on global metabolite profiles within the airways to distinguish overall changes between exposure and sex. Prior to analysis, we stratified males and females into separate groups considering previous studies reporting sex differences in response to ozone exposure (Cho et al., 2019; Yaeger et al., 2021). Additionally, we assessed the median relative standard deviation in metabolite abundance within the saline and FA controls of both sexes to rule out the potential influence of cycle stage in affecting variance among females (Supplementary File 1). We observed minor differences between median RSD values in the control groups, which were 29.9% in males and 27.5% in females. To determine differences between exposure in male mice, PCA revealed distinct clustering between HDM-sensitized mice exposed to ozone (HDM+O<sub>3</sub>) and males sensitized to HDM without ozone challenge (HDM), where 32.9% of the overall variance explained by the first principal component was sufficient to discriminate each of these groups (Supplementary Figure 2). Interestingly, PCA did not result in clustering between the HDM and the HDM + O<sub>3</sub> groups in females, with 35.6% of the overall variance explained by the first principal component leading to marginal separation between each group. Likewise, the results of 1-way ANOVA comparing changes in individual metabolite abundance for all groups relative to control male and female mice supported the results of PCA. A greater number of metabolites were significantly altered in males than females for all treatment groups except mice exposed to ozone alone (Supplementary File 1 and Table 4). Taken together, these results suggested that combined HDM + O<sub>3</sub> exposure altered global metabolite profiles in males more than in females relative to control mice. Therefore, we focused most our subsequent analyses on comparing the combined HDM + O<sub>3</sub> exposure group versus the control mice to discern metabolite classes and individual metabolites attributable to clustering in our PCA.



The results of the significance tests and corresponding fold-changes for all metabolites were combined in ChemRICH software to determine changes in overall metabolite classes. For both male and female mice, ChemRICH analysis showed that numerous lipid classes, dipeptides, and amino acids were significantly altered following combined HDM + O<sub>3</sub> exposure relative to controls (Table 1 and Supplementary Table 5 and Figure 3). However, the composition of significantly altered metabolites within each class varied widely between sexes (Supplementary Table 5). For membrane lipids, specifically for unsaturated PC and unsaturated PE, we found sexual dimorphism in response to HDM + O<sub>3</sub> exposure. Although for male mice, we found 29 upregulated and 26 downregulated PCs and PEs out of 143 identified lipid species, this ratio was very different for female mice with 49 upregulated and only 12 downregulated membrane lipid species (Supplementary Table 5). For combined HDM + O<sub>3</sub> exposure versus controls, male mice showed 104 out of 130 triacylglycerides to be significantly decreased (Supplementary Table 5), along with significant decreases for 21 out of 31 sphingomyelins (Table 1). Conversely, female mice showed only 43/130 triacylglycerides to be decreased (Supplementary Table 5), and only 10/31 sphingomyelins were found decreased under combined HDM + O<sub>3</sub> exposure versus controls (Table 1).

For oxidized and non-oxidized glycosylceramides (oxGlcCer and GlcCer), we found 15/17 lipids to be increased in contents in females, but only 6/17 glycosylceramides were found differently regulated in males when comparing HDM + O<sub>3</sub> exposure versus controls (Table 1). Of the 17 GlcCer species identified, 6 of these were significantly increased in the males sensitized to HDM and exposed to ozone relative to controls (Figure 2A and Supplementary Table 6). Strikingly, 15/17 GlcCer species were significantly increased following combined HDM sensitization and ozone exposure in females, 8 of which were from 2- to 32-fold higher in abundance relative to control-treated mice (Figure 2B and Supplementary Table 6). Digalactosylceramide 34:1 and dihexosylceramide 34:1 were the 2 GlcCer species with the greatest relative increases in the combined exposure group, which was also observed in males. In addition, several GlcCer species containing very long-chain fatty acids (VLCFAs) were uniquely increased in females but not in males marked by more than 2-fold higher abundance in the combined exposure group relative to control-treated mice (Figure 2). Similar to the results of ChemRICH analysis, GlcCer species were also increased in HDM-sensitized males and females that did not undergo ozone exposure (Supplementary Figs. 4 and 6). However, HDM sensitization alone did not result in extensive decreases in SMs and ceramides in contrast to combined HDM sensitization and ozone exposure. Notably, increases in GlcCer species were present in both males and females in HDM-sensitized mice in the absence of ozone exposure, but HDM sensitization alone did not elicit as many decreases in other sphingolipid subclasses and membrane lipids that were characteristic of the combined exposure groups (Supplementary Figure 5). These results aligned with changes in sphingolipid subclass ratios, which corresponded to overall increases in unsaturated ceramides relative to unsaturated sphingomyelins as well as unsaturated glycosylceramides relative to unsaturated ceramides in the combined exposure groups relative to control mice (Supplementary Figure 7). Importantly, these changes were present in both male and female mice, indicating increased conversion of sphingomyelin to ceramide. Overall, these results demonstrated a shift in composition of sphingolipid abundance that favored a higher proportion of

glycosphingolipids in the combined exposure group relative to control mice.

### Sphingolipid correlation structure varies by sex

Because we had determined that sphingolipids showed interesting sexual dimorphism in female and male mice, specifically in relation to opposite trends in ratios between sphingolipid subclasses, we set out to determine the numerical associations between individual sphingolipids across all treatments. Metabolite: metabolite correlation analysis tests the dependence between metabolite ratios that are altered in response to specific treatments, which in turn can reflect differences in metabolic flux along pathways and diverting enzymatic nodes. Results of comprehensive correlation analysis for all metabolites involved in sphingolipid synthesis further supported the differences between males and females in sphingolipid metabolism (Figure 3). In males, correlation coefficients were consistently lower for all sphingolipid subclasses than in females. Although ceramide levels were associated with glycosylceramides in both male and female mice, we found a large increase of statistically significant correlations in females compared with males. Conversely, females exhibited significant associations between nearly all GlcCer species and the corresponding GlcCer precursors UDP-acetylgalactosamine, UDP-galactose, N-acetylneuraminic acid, and N-glycolylneuraminic acid (Figure 3B). In contrast, in males only half of the individual GlcCer species displayed positive correlations with GlcCer precursors (Figure 3A). Interestingly, the nutrient choline was positively associated with all sphingomyelins and most ceramides for females, whereas males showed negative correlations with hexosylceramides or lack of significance for most other sphingolipids.

### Airway resistance is synergistically increased following combined HDM and ozone in males but not in females

We conducted pulmonary function testing, cell differentials, and histological analysis to determine how sex-dependent increases in glycosphingolipids related to physiological and cellular outcomes following combined HDM-sensitization and ozone exposure. Increases in BALF neutrophils, eosinophils, and lymphocytes were primarily driven by HDM sensitization rather than ozone exposure in both males and females. This finding was expected based on previous studies detailing extensive immune cell influx in BALF following similar HDM-sensitization protocols (Castaneda and Pinkerton, 2016; Mack et al., 2019) (Figs. 4A and 4B). However, we also observed a statistically significant increase in the number of BALF eosinophils in the HDM + O<sub>3</sub> exposure group relative to HDM sensitization alone, which was not observed in female mice (Figure 4A). We did not observe any statistically significant changes in the number of eosinophils or lymphocytes relative to control-treated mice in animals exposed to ozone in the absence of HDM-sensitization. However, BALF neutrophils were increased in female mice exposed to ozone alone and approached statistical significance ( $p = .06$ ) (Figure 4B).

Methacholine challenges conducted within each treatment group resulted in marked differences in airway resistance between treatment and sex. HDM sensitization alone was sufficient to increase the response to methacholine relative to control-treated mice at comparable doses of methacholine as expected (Figs. 4C and 4D). Interestingly, combined HDM + O<sub>3</sub> exposure exhibited a synergistic effect on airway resistance in males, which was not present in females (Figs. 4C and 4D). Airway resistance at a dose of 0.5 mg/ml methacholine was approximately 4-fold greater in the combined exposure group

**Table 1.** Glycosphingolipids are substantially increased in sensitized females exposed to ozone

Cluster name	Class size	q value	Male		q value	Female	
			Increased	Decreased		Increased	Decreased
OxCer	4	1.1E-03	0	3	0.12	1	0
OxGlcCer	5	1	0	0	4.8E-05	4	0
OxSM	3	0.27	0	1	0.099	0	1
Saturated SM	6	2.8E-04	0	3	0.096	0	0
Unsaturated Cer	17	0.082	2	2	1.9E-03	1	3
Unsaturated GlcCer	12	1.5E-03	6	0	3.0E-14	11	0
Unsaturated SM	25	2.6E-11	0	18	1.6E-06	0	10

List of sphingolipid classes comparing the abundance in airways from sensitized, ozone-exposed males and females relative to control mice using chemical similarity enrichment analysis (ChemRICH). The number of individual metabolites contained within a group is indicated by class size. Sphingolipids that are increased or decreased between groups correspond to individual species with a fold-increase or decrease greater than 2. *q* values for each cluster were calculated using a Kolmogorov-Smirnov test followed by Benjamini-Hochberg adjustment for false-discovery rate (FDR), and  $q < 0.05$  was used as the threshold for statistical significance. The full list of metabolite classes analyzed by ChemRICH included in [Supplementary Table 5](#).

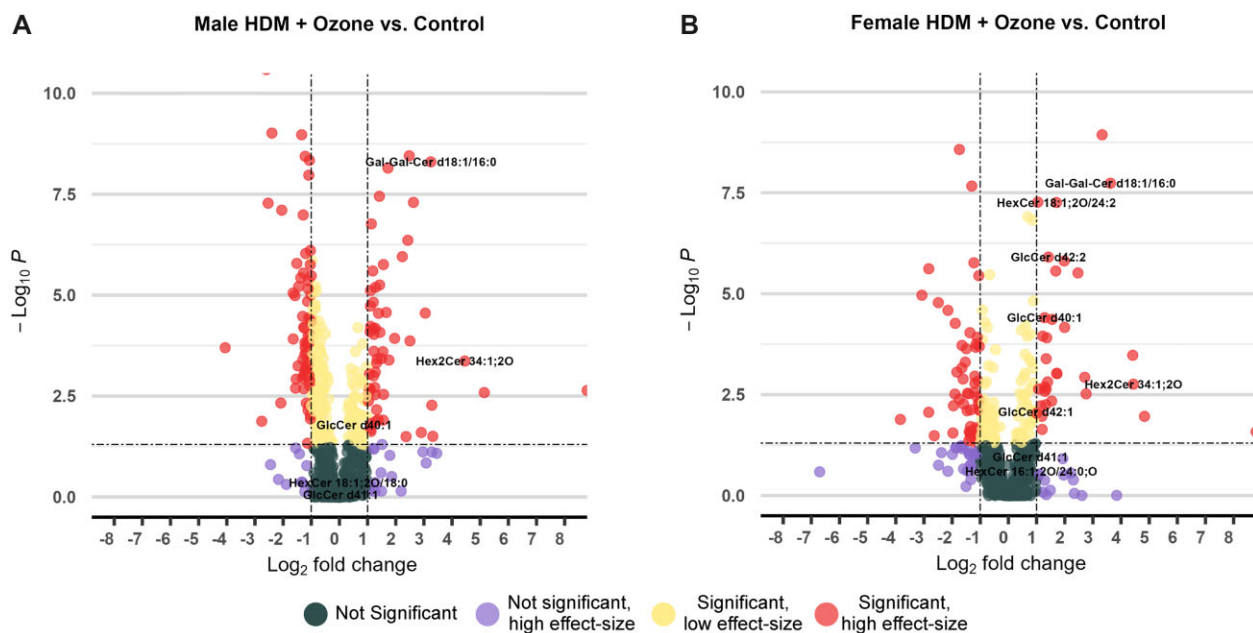


**Figure 2.** The number and magnitude of glycosphingolipids increased in sensitized and exposed females is greater than in males. A and B, Volcano plots displaying significantly altered metabolites in sensitized males and females exposed to ozone relative to vehicle control, respectively. A fold change cutoff of 2 or greater is defined as a high-effect size, and  $p < .05$  is used as a cutoff for statistical significance. *p* values were calculated by 1-way ANOVA with Tukey's *post hoc* analysis.

compared with either HDM sensitization alone, ozone exposure alone, or vehicle in males (Figure 4C). Higher levels of methacholine resulted in nearly complete occlusion of the airways in male mice. In contrast, airway resistance in females between the combined exposure group and HDM sensitization alone at 0.5 mg/ml methacholine was not significantly different compared with the measured resistance in vehicle-treated mice (Figure 4D). Additionally, we did not observe any statistically significant changes in airway resistance at baseline between either the combined exposure group or HDM alone in both sexes.

Histological analysis of lung sections stained with H&E further corroborated the differences in AHR observed from pulmonary function testing. Male mice in the HDM + O<sub>3</sub> exposure group displayed extensive inflammation of proximal airways, thickening of the airway epithelium, and airway narrowing compared with either HDM sensitization or ozone exposure alone (Figure 5A). Conversely, combined HDM + O<sub>3</sub> exposure demonstrated less pronounced morphological changes in the proximal airways of female mice (Figure 5B). However, the combined exposure did not

appear to exhibit sexual dimorphism in goblet cell hyperplasia, which was evidenced by AB/PAS staining in males and in females (Supplementary Figure 8). Overall, males that were sensitized to HDM and exposed to ozone experienced increased eosinophilia, greater airway obstruction, and more severe AHR than females relative to control-treated mice.

### Sex differences in glycosphingolipid abundance are associated with eosinophilia and AHR

Lastly, we used linear regression to characterize associations between glycosphingolipid abundance and airway resistance as well as eosinophilia that would establish the importance of sex differences in glycosphingolipids and their implications in physiological differences within our study. Interestingly, glycosphingolipid abundance was positively associated with both BALF eosinophils and airway resistance in males and females (Figure 6 and Supplementary Table 7). Male mice displayed statistically significant associations between 6 individual glycosphingolipid species and BALF eosinophils, whereas 11 glycosphingolipids

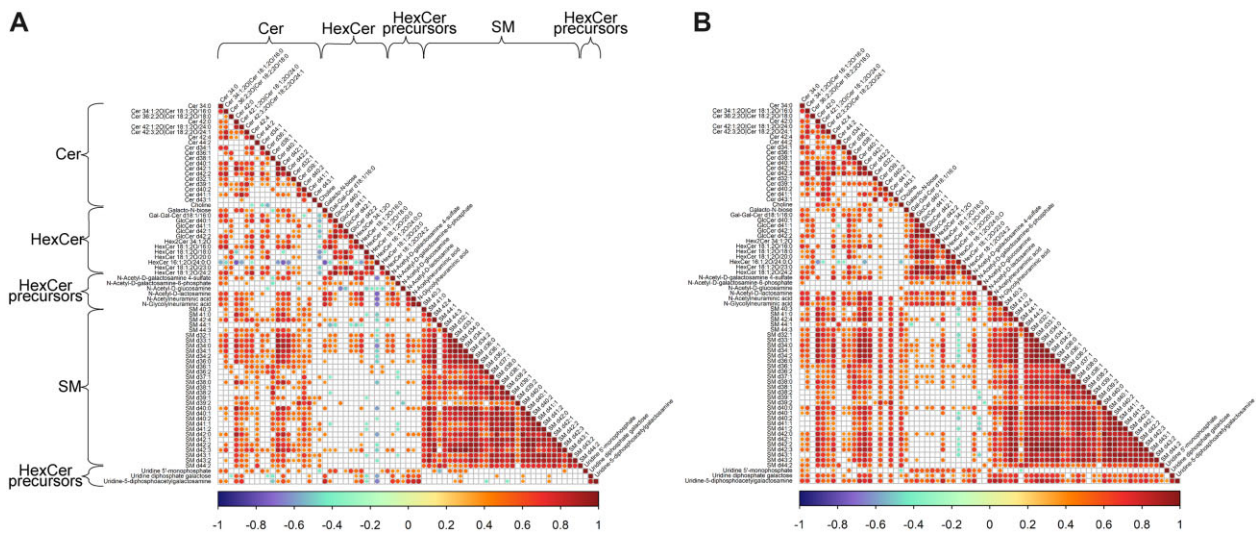


**Figure 3.** Correlations between glycosphingolipids and other sphingolipid species are stronger in females than in males. A and B, Correlation matrices indicating Pearson correlation coefficients between individual sphingolipids in sensitized males and females exposed to ozone relative to vehicle control, respectively. Correlations that are not statistically significant ( $p > .05$ ) are left blank in each matrix. Locations containing subclasses of sphingolipids are indicated by labels across the rows and columns of (A), the order of which is unchanged in (B).

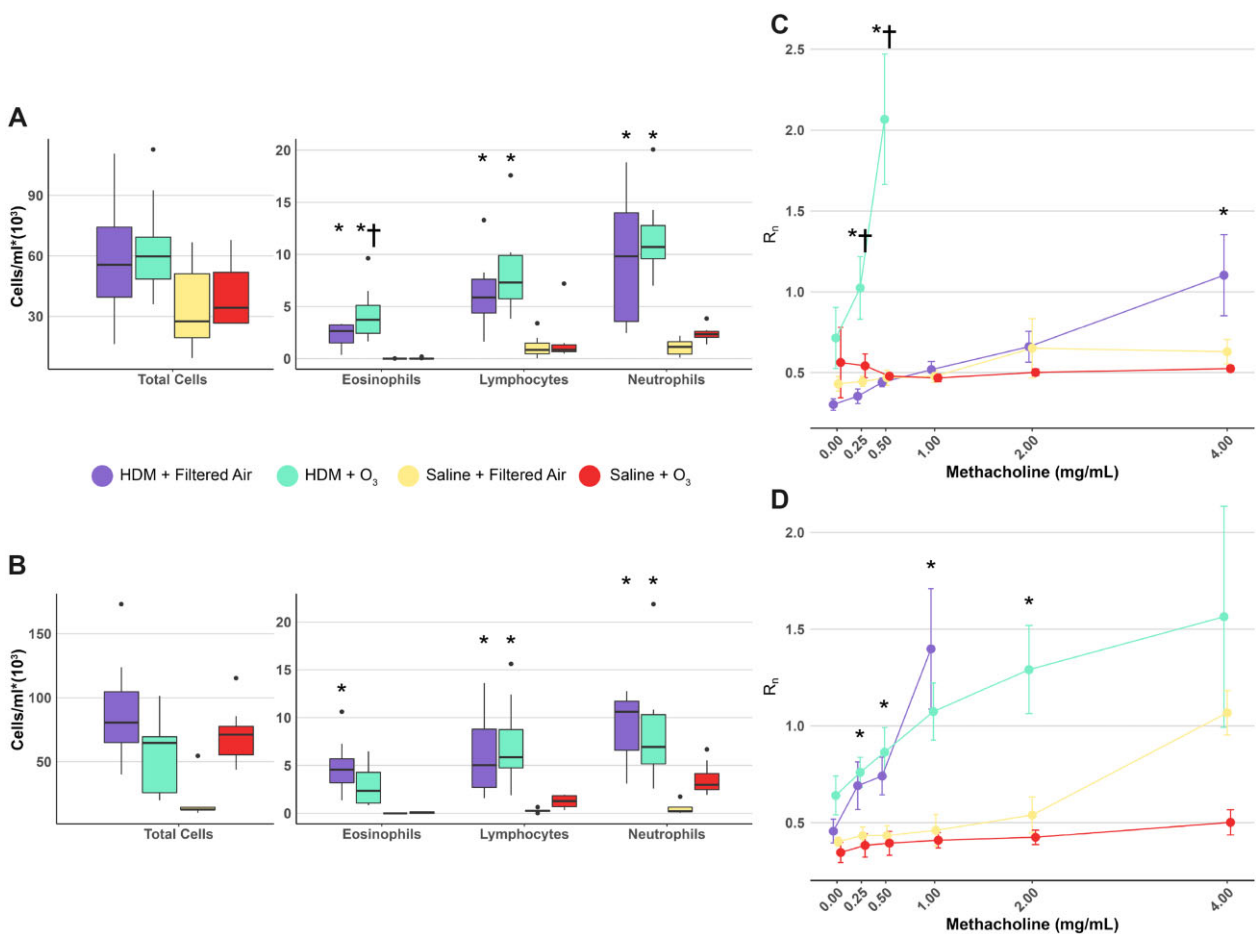


**Figure 4.** Ozone exposure synergistically increases AHR in HDM-sensitized male mice. Total BALF cells, leukocyte numbers, and methacholine dose-response curves from males (A and C) and females (B and D), where  $R_n$  is the Newtonian resistance calculated based on a constant phase model expressed in units of  $\text{cmH}_2\text{O} \cdot \text{min}/\text{mL}$ . \* $p < .05$  relative to control and † $p < .05$  relative to HDM + filtered air-treated mice.  $p$  values were calculated by 1-way ANOVA with Tukey's *post hoc* analysis.



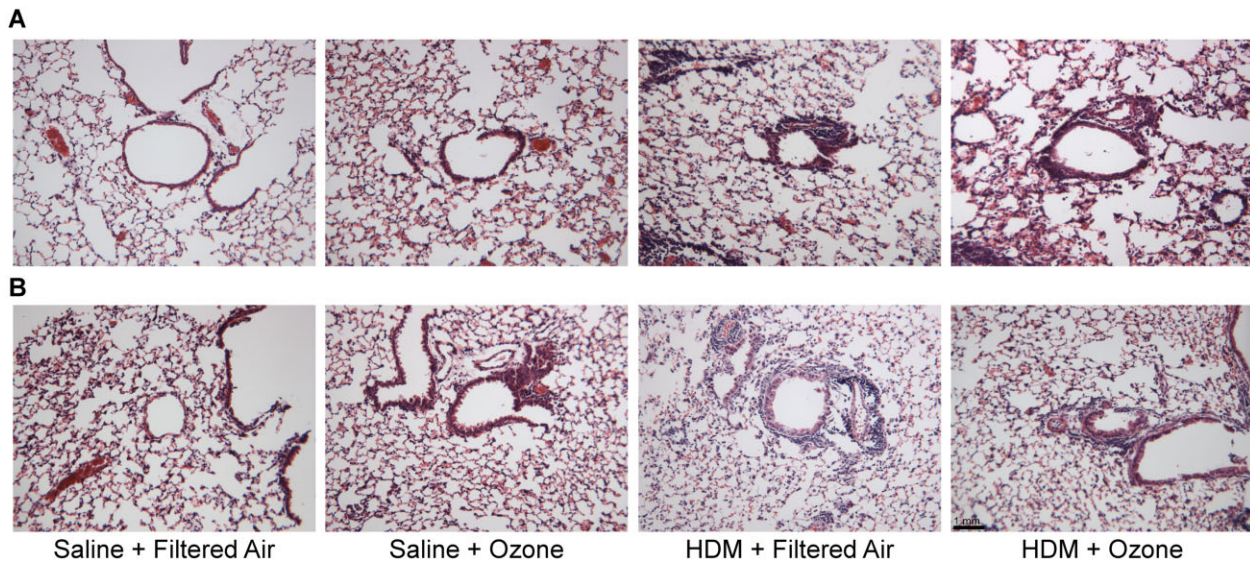


**Figure 5.** Ozone enhances airway inflammation in HDM-sensitized male mice. Representative images of H&E slides detailing morphology of proximal airways in (A) male and (B) female mice within each treatment group.  $N=3/\text{group}$ ,  $10\times$  magnification, bar = 1 mm.

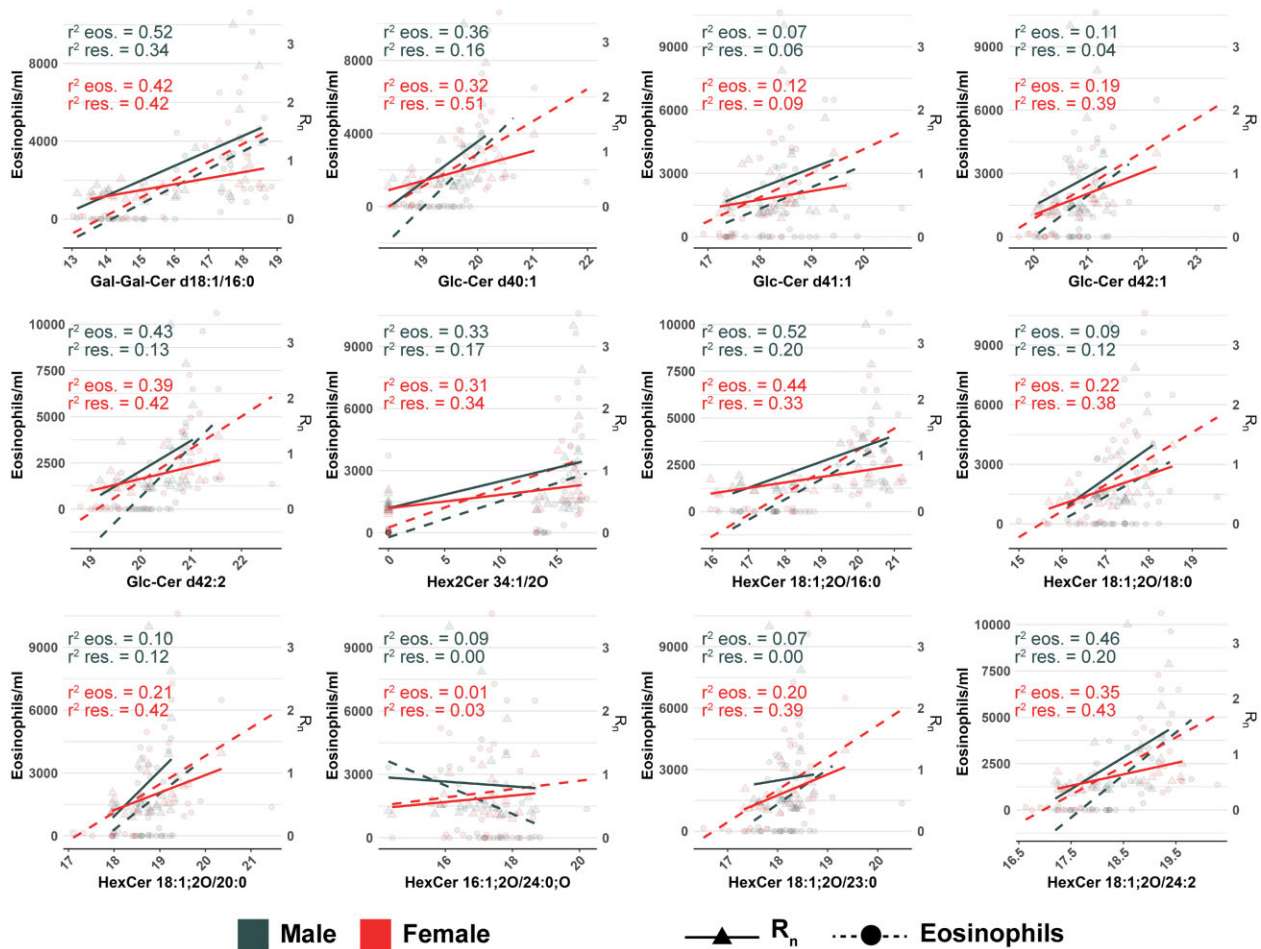


**Figure 6.** Eosinophilia and airway resistance are positively associated with glycosphingolipid abundance. Regression analysis between individual glycosphingolipid species and either BALF eosinophil counts, or  $R_n$  values obtained from pulmonary function testing. Solid lines and dotted lines correspond to the regression lines for resistance values (triangles) and eosinophil counts (circles), respectively. The coefficient of determination ( $R^2$ ) is included for both male and female mice, and statistically significant relationships are included in [Supplementary Table 7](#). Values were based on results of a simple linear regression model, and significant associations were based on  $p < .05$ .



were significantly associated with BALF eosinophils in female mice. In general,  $R^2$  values were comparable between significant associations in males and females, which ranged from 0.33 to 0.52 for males and 0.19 to 0.44 for females (Figure 6 and Supplementary Table 7). In contrast, glycosphingolipid abundance was a poorer predictor of airway resistance in males than in females. Only 3 individual glycosphingolipids were associated with airway resistance in males compared with 10 in females. Furthermore, the proportion of variance explained by these significant associations was greater in females where  $R^2$  values ranged from 0.33–0.51 compared with 0.20–0.34 in male mice (Figure 6 and Supplementary Table 7). These results demonstrated that glycosphingolipid abundance was associated with characteristics of asthma in both male and female mice, but the abundance of glycosphingolipids was a better indicator of AHR in females compared with males.

## Discussion

Our study implicates glycosphingolipids in mitigating ozone-induced exacerbations in allergic asthma characteristics. The results of our study expand upon previous findings that have detailed the role of sphingolipids in modulating characteristics of allergic asthma by utilizing a well-established mouse model that incorporates a physiologically relevant route of allergic sensitization (James et al., 2021; Oyeniran et al., 2015; Park and Im, 2019). However, this is the first study, to our knowledge, that has examined the effects of ozone in terms of precipitating changes in sphingolipid metabolism in tandem with classical characteristics associated with exacerbation in allergic asthma. Furthermore, the potential involvement of glycosphingolipids in allergic asthma remains largely understudied. Our findings link ozone exposure to a likely induction of acid sphingomyelinase-mediated breakdown of sphingomyelin and to the upregulation of glycosphingolipids, which is supported by the increased conversion of sphingomyelins to ceramides and ceramides to glycosylceramides observed in our study. Through sampling of microdissected tissue, we isolated changes in glycosphingolipids to the proximal airways, which is the primary lung region affected by ozone exposure and that is predominantly involved in asthma pathology. Importantly, we observed that AHR, airway obstruction, and immune cell influx were most prominent in male mice, analogous to previous reports indicating distinctive responses to ozone based on sex (Birukova et al., 2019; Cho et al., 2019).

The overall sex differences in global metabolite profiles following ozone exposure were reflected by unsupervised multivariate analysis. Clear separation using PCA was achieved between HDM-sensitized male mice acutely exposed to ozone and either animals who only received HDM or did not undergo HDM sensitization (Supplementary Figure 2A). Conversely, no separation was observed between either of the HDM-sensitized groups in females and groups that did not receive HDM. This finding was indicative of the lack of drastic changes in females with respect to abundance of metabolite classes between treatment groups (Supplementary Figure 2B). Over half of all identified lipids were comprised of TGs, PCs, and PEs which therefore likely dominated clustering differences observed in PCA and the majority of significantly altered metabolites based on univariate analysis (Supplementary Tables 2 and 5).

ChemRICH analysis supported the results of multivariate statistics. ChemRICH set enrichments identified significant changes in membrane and storage lipids following combined HDM

sensitization and ozone exposure relative to control mice, which also exhibited clear sex differences for specific lipid classes (Supplementary Table 5). Interestingly, only unsaturated PC- and PE-membrane lipids showed large differential regulation after HDM + O<sub>3</sub> exposure, but not saturated membrane lipids. This effect was also stronger in females than in males. Unsaturated membrane lipids strongly contribute to elasticity and fluidity of membrane, hence assisting the overall lung compliance. Therefore, the higher degree of unsaturated PCs and PEs in female than in male mice may further contribute to the greater resistance against HDM + O<sub>3</sub> stress in females. This effect may also imply increased repair of the airway epithelium following ozone exposure in females compared with males (Wright et al., 2000; Zehethofer et al., 2015). For male mice, trends in decreasing PC- and PE-lipid abundance in the combined HDM and ozone group may reflect increases in apoptosis of airway epithelial cells as well as oxidation of lipids in lung surfactant (Murphy et al., 2014; Uhlson et al., 2002).

We found large changes in sphingolipid abundance in response to HDM + O<sub>3</sub> treatment. For males, 21/31 identified SMs were decreased and 6/17 glycosphingolipids were found increased (Table 1). This response contrasted the observed changes in females where 10/31 SMs were decreased, but 15/17 glycosphingolipids were increased, concomitant with a decrease in ceramide abundance. Decreases in SM abundance coupled with increases in glycosphingolipids may elude to increased formation of sphingolipids from recycling and salvage of SM within the cell membrane (Smith and Schuchman, 2008). Importantly, these changes in abundance were likely independent of *de novo* sphingolipid synthesis, which is supported by the lack of changes in serine and palmitic acid represented in our metabolomics analysis as well as changes in ratios between sphingolipid subclasses (Zhang et al., 2019b) (Supplementary Figure 7). Following cleavage of SM from the cell membrane, ceramide species are formed and either directly participate in cell signaling during apoptosis, undergo modification into glucosyl- and galactosylceramides, or undergo breakdown into sphingosine 1-phosphate (Gault et al., 2010; James et al., 2021). Unfortunately, we were unable to detect sphingosine 1-phosphate in this study to evaluate the contributions of this metabolite, which is an inherent limitation of using untargeted assays to detect metabolites with low abundance such as sphingosine 1-phosphate. Nonetheless, the observed increases in glycosphingolipids in both males and females as well as the increased ratio of glycosylceramides to ceramide may correspond to increased activity of UDP-galactose and UDP-glucose ceramide transferases, which would allude to increased GlcCer-mediated signaling compared with ceramide-mediated signaling events (Ishibashi et al., 2013; Sprong et al., 1998) (Supplementary Figure 7). Additionally, the results of our correlation analysis indicate that females may exhibit tighter control over the flux between ceramides and glycosphingolipids than males, which is depicted by stronger overall associations between these sphingolipid subclasses in females than in males (Figure 3).

Differences in glycosphingolipid signaling may explain the discrepancies in AHR, airway obstruction, and immune cell influx between males and females. Following combined HDM + O<sub>3</sub> exposure, males but not females displayed synergistically increased AHR compared with either HDM sensitization or ozone exposure alone (Figs. 4C and 4D). Combined exposure in males but not in females also led to significantly increased BALF eosinophils relative to HDM sensitization alone (Figs. 4A and 4B). These outcomes were consistent with the results of histological analysis

that showed greater airway inflammation and thickening of the airway epithelium in males compared with females (Figs. 5A and 5B). Importantly, glycosphingolipid abundance was positively associated with airway resistance and BALF eosinophils in both male and female mice (Figure 6 and Supplementary Table 7). However, 10 individual glycosphingolipid species displayed a significant association with airway resistance in female mice compared with only 3 species in males, which was also marked by stronger associations in females ( $R^2 = 0.33\text{--}0.51$ ). Therefore, glycosphingolipids significantly upregulated in airways of female mice may serve to protect against severe AHR, airway inflammation, and increased eosinophil recruitment, which is less pronounced in males. Intriguingly, glycosphingolipids act as ligands that modulate natural killer T (NKT) cell activation, the effects of which have been linked to regulation of airway inflammation and AHR (Chen et al., 2021; Gorska, 2017; Pichavant et al., 2008). Furthermore, administering the synthetic  $\alpha$ -galactosylceramide analog KRN7000 was previously reported to mitigate airway inflammation in model of obese asthma in mice, which was most efficacious in obese mice that also received allergen (Chen et al., 2021). These findings suggest that NKT cell activity induced by glycosphingolipids may be especially important in regulation of severe asthma phenotypes, which is recapitulated by the combined allergen and ozone exposure used in our study.

In addition to class abundance and associations between physiological outcomes, the enrichment of glycosphingolipids containing specific lengths of fatty acyl-chains alludes to differential patterns of NKT cell activity. Differential NKT cell activity may contribute to the sex differences observed in our study. Multiple glycosphingolipids containing VLCFAs (>22 carbon atoms) were increased 2-fold or greater in females but not in males under HDM + O<sub>3</sub> exposure (Figs. 2A and 2B and Supplementary Table 5). Previous findings have demonstrated a positive association between increasing acyl chain length and GlcCer-induced NKT cell activity. These observations are based on *in vitro* experiments utilizing cultured NKT cells that show the greatest extent of activation upon administration of galactosylceramides containing VLCFAs, which is decreased with shortening acyl chain length (Kawano et al., 1997). Taken together, the observed increases in glycosphingolipids with VLCFAs suggest that NKT cell activation is greater in HDM-sensitized females than in males upon ozone exposure, which may prevent severe outcomes in females.

The effects of ozone exposure on exacerbating allergic asthma are demonstrated by a variety of animal models and epidemiologic studies in humans. Airway inflammation and AHR in animal models as well as previous metabolomics analyses in humans following ozone exposure indicate that ozone-induced exacerbations in asthma may be mediated in part by perturbations in sphingolipid metabolism and signaling (Bao et al., 2018; Cheng et al., 2018; Miller et al., 2016; Williams et al., 2008). However, no studies to date have evaluated the effects of ozone exposure on altering sphingolipid metabolism in relation to exacerbation of allergic asthma. The objective of our study was to examine ozone-induced changes in sphingolipid metabolism using a mouse model of allergic asthma. Our model consisted of intranasal instillation of HDM during both the sensitization and challenge phase, with each challenge followed exposure to 0.5 ppm ozone for 6 h each day. This route of allergen administration as well as the concentration and duration of ozone exposure we selected mimics the route of allergen sensitization in humans and considers species differences in susceptibility to ozone. The duration of ozone exposure used in our study also accounts for

diurnal variation in ozone concentrations. Therefore, the results of this study may provide insights into mechanisms underlying ozone-induced asthma exacerbations in humans.

## Conclusions

We found an interesting association between glycosphingolipid abundance and corresponding changes in AHR, airway inflammation, and immune cell recruitment within the airways. This finding warrants further investigation of glycosphingolipids within the lung. Established mechanisms of sphingolipid signaling in allergic asthma have primarily been based on the functions of ceramides and sphingosine 1-phosphate in mediating immune responses and AHR associated with asthma (James et al., 2021; Oyeniran et al., 2015; Yang and Uhlig, 2011). However, our findings that glycosphingolipid abundance is significantly altered by combined allergen and ozone exposure which is significantly associated with airway resistance and eosinophilia demonstrates potential mechanisms underlying allergic asthma involving glycosphingolipid signaling. In comparison to previous work, our dissections allowed for greater spatial resolution of metabolomic responses within the lung. Our approach analyzing microdissected lung airways captures changes in sphingolipids within both the primary target of ozone exposure and region implicated in asthma. In contrast, previous measurements of sphingolipids in mouse models of asthma have sampled BALF and homogenized whole lung tissue (James et al., 2021), which limit the ability to isolate changes in abundance to specific lung regions.

Overall, our analysis provides the basis for future experiments determining the spatial changes in glycosphingolipid metabolism that contribute to ozone-induced exacerbations in asthma. Our work also identifies additional targets for development of therapeutics used to treat various subtypes of asthma.

## Supplementary data

Supplementary data are available at *Toxicological Sciences* online.

## Acknowledgments

We thank the undergraduate student members of the Van Winkle and Pinkerton laboratories for their assistance with lung microdissection and support during sample collection. We also thank Jalen Chang, an undergraduate student in the Van Winkle laboratory, for his contributions to the staining and analysis of the H&E and AB/PAS slides prepared for this study.

## Author contributions

N.C.S., L.S.V.W., and O.F. prepared the manuscript; N.C.S., L.S.V.W., and P.C.E. developed the experimental design for the study; N.C.S., V.J.B., M.C.D., and P.C.E. performed the animal experiments and tissue collection; N.C.S. conducted data processing, statistics, and analysis; and all authors contributed to editing the manuscript.

## Funding

L.S.V.W. was supported by the National Institutes of Health (R21 ES030276). N.C.S. and V.J.B. received support from T32 ES007059 and M.C.D., N.C.S. and V.J.B. were supported by T32 HL007013. The metabolomic damage by ozone was funded by the National Institutes of Health (U19 AG023122 to O.F.)

## Declaration of conflicting interests

The authors declared no potential conflicts of interest with respect to the research, authorship, and/or publication of this article.

## References

- American Lung Association. (2021). *State of the Air Report 2021*. American Lung Association, Chicago, IL.
- Ammit, A. J., Hastie, A. T., Edsall, L. C., Hoffman, R. K., Amrani, Y., Krymskaya, V. P., Kane, S. A., Peters, S. P., Penn, R. B., Spiegel, S., et al. (2001). Sphingosine 1-phosphate modulates human airway smooth muscle cell functions that promote inflammation and airway remodeling in asthma. *FASEB J.* **15**, 1212–1214.
- Bao, A., Yang, H., Ji, J., Chen, Y., Bao, W., Li, F., Zhang, M., Zhou, X., Li, Q., and Ben, S. (2017). Involvements of p38 MAPK and oxidative stress in the ozone-induced enhancement of AHR and pulmonary inflammation in an allergic asthma model. *Respir. Res.* **18**, 1–12.
- Bao, W., Zhang, Y., Zhang, M., Bao, A., Fei, X., Zhang, X., and Zhou, X. (2018). Effects of ozone repeated short exposures on the airway/lung inflammation, airway hyperresponsiveness and mucus production in a mouse model of ovalbumin-induced asthma. *Biomed. Pharmacother.* **101**, 293–303.
- Barupal, D. K., and Fiehn, O. (2017). Chemical Similarity Enrichment Analysis (chemRICH) as alternative to biochemical pathway mapping for metabolomic datasets. *Sci. Rep.* **7**, 14567.
- Birukova, A., Cyphert-Daly, J., Cumming, R. I., Yu, Y. R., Gowdy, K. M., Que, L. G., and Tighe, R. M. (2019). Sex modifies acute ozone-mediated airway physiologic responses. *Toxicol. Sci.* **169**, 499–510.
- Böll, S., Ziemann, S., Ohl, K., Klemm, P., Rieg, A. D., Gulbins, E., Becker, K. A., Kamler, M., Wagner, N., Uhlig, S., et al. (2020). Acid sphingomyelinase regulates TH2 cytokine release and bronchial asthma. *Allergy* **75**, 603–615.
- Bonini, P., Kind, T., Tsugawa, H., Barupal, D. K., and Fiehn, O. (2020). Retip: retention time prediction for compound annotation in untargeted metabolomics. *Anal. Chem.* **92**, 7515–7522.
- Cajka, T., and Fiehn, O. (2016). Increasing lipidomic coverage by selecting optimal mobile-phase modifiers in LC-MS of blood plasma. *Metabolomics* **12**, 1–11.
- Castaneda, A. R., and Pinkerton, K. E. (2016). Investigating the effects of particulate matter on house dust mite and ovalbumin allergic airway inflammation in mice. *Curr. Protoc. Toxicol.* **68**, 18 18 11–18 18 18.
- Chen, Y., Zhu, Y., Su, G., Yang, W., Zhao, Y., Lu, W., and Zhang, J. (2021). Krm7000 reduces airway inflammation via natural killer T cells in obese asthmatic mice. *Inflammation* **44**, 1982–1992.
- Cheng, W. Y., Duncan, K. E., Ghio, A. J., Ward-Caviness, C., Karoly, E. D., Diaz-Sanchez, D., Conolly, R. B., and Devlin, R. B. (2018). Changes in metabolites present in lung-lining fluid following exposure of humans to ozone. *Toxicol. Sci.* **163**, 430–439.
- Cho, Y., Abu-Ali, G., Tashiro, H., Brown, T. A., Osgood, R. S., Kasahara, D. I., Huttenhower, C., and Shore, S. A. (2019). Sex differences in pulmonary responses to ozone in mice. Role of the microbiome. *Am. J. Respir. Cell Mol. Biol.* **60**, 198–208.
- Gault, C. R., Obeid, L. M., and Hannun, Y. A. (2010). An overview of sphingolipid metabolism: from synthesis to breakdown. *Adv. Exp. Med. Biol.* **688**, 1–23.
- Gendron, D. R., Lecours, P. B., Lemay, A.-M., Beaulieu, M.-J., Huppé, C.-A., Lee-Gosselin, A., Flamand, N., Don, A. S., Bissonnette, É., Blanchet, M.-R., et al. (2017). A phosphorylatable sphingosine analog induces airway smooth muscle cytoostasis and reverses airway hyperresponsiveness in experimental asthma. *Front. Pharmacol.* **8**, 78.
- Gorska, M. M. (2017). Natural killer cells in asthma. *Curr. Opin. Allergy Clin. Immunol.* **17**, 50–54.
- Guarnieri, M., and Balmes, J. R. (2014). Outdoor air pollution and asthma. *The Lancet* **383**, 1581–1592.
- Herring, M. J., Putney, L. F., St George, J. A., Avdalovic, M. V., Schelegle, E. S., Miller, L. A., and Hyde, D. M. (2015). Early life exposure to allergen and ozone results in altered development in adolescent rhesus macaque lungs. *Toxicol. Appl. Pharmacol.* **283**, 35–41.
- Hu, S.-C., Ben-Jebria, A., and Ultman, J. (1994). Longitudinal distribution of ozone absorption in the lung: effects of respiratory flow. *J. Appl. Physiol.* **77**, 574–583.
- Ishibashi, Y., Kohyama-Koganeya, A., and Hirabayashi, Y. (2013). New insights on glucosylated lipids: metabolism and functions. *Biochim. Biophys. Acta* **1831**, 1475–1485.
- James, B. N., Oyeniran, C., Sturgill, J. L., Newton, J., Martin, R. K., Bieberich, E., Weigel, C., Maczys, M. A., Palladino, E. N. D., Lownik, J. C., et al. (2021). Ceramide in apoptosis and oxidative stress in allergic inflammation and asthma. *J. Allergy Clin. Immunol.* **147**, 1936–1948.e9.
- Kawano, T., Cui, J., Koezuka, Y., Toura, I., Kaneko, Y., Motoki, K., Ueno, H., Nakagawa, R., Sato, H., Kondo, E., et al. (1997). CD1d-restricted and TCR-mediated activation of va14 NKT cells by glycosylceramides. *Science* **278**, 1626–1629.
- Kim, H. I., Kim, H., Shin, Y. S., Beegle, L. W., Jang, S. S., Neidholdt, E. L., Goddard, W. A., Heath, J. R., Kanik, I., and Beauchamp, J. L. (2010). Interfacial reactions of ozone with surfactant protein B in a model lung surfactant system. *J. Am. Chem. Soc.* **132**, 2254–2263.
- Koelmel, J. P., Kroeger, N. M., Gill, E. L., Ulmer, C. Z., Bowden, J. A., Patterson, R. E., Yost, R. A., and Garrett, T. J. (2017). Expanding lipidome coverage using LC-MS/MS data-dependent acquisition with automated exclusion list generation. *J. Am. Soc. Mass Spectrom.* **28**, 908–917.
- Mack, S., Shin, J., Ahn, Y., Castaneda, A. R., Peake, J., Fulgar, C., Zhang, J. J., Cho, Y. H., and Pinkerton, K. E. (2019). Age-dependent pulmonary reactivity to house dust mite allergen: a model of adult-onset asthma? *Am. J. Physiol. Lung Cell. Mol. Physiol.* **316**, L757–L763.
- Miller, D. B., Ghio, A. J., Karoly, E. D., Bell, L. N., Snow, S. J., Madden, M. C., Soukup, J., Cascio, W. E., Gilmour, M. I., and Kodavanti, U. P. (2016). Ozone exposure increases circulating stress hormones and lipid metabolites in humans. *Am. J. Respir. Crit. Care Med.* **193**, 1382–1391.
- Murphy, S. R., Oslund, K. L., Hyde, D. M., Miller, L. A., Van Winkle, L. S., and Schelegle, E. S. (2014). Ozone-induced airway epithelial cell death, the neurokinin-1 receptor pathway, and the postnatal developing lung. *Am. J. Physiol. Lung Cell. Mol. Physiol.* **307**, L471–L481.
- Mustafa, M. G. (1990). Biochemical basis of ozone toxicity. *Free Radic. Biol. Med.* **9**, 245–265.
- Oyeniran, C., Sturgill, J. L., Hait, N. C., Huang, W.-C., Avni, D., Maceyka, M., Newton, J., Allegood, J. C., Montpetit, A., Conrad, D. H., et al. (2015). Aberrant ORM (yeast)-like protein isoform 3 (ORMDL3) expression dysregulates ceramide homeostasis in cells and ceramide exacerbates allergic asthma in mice. *J. Allergy Clin. Immunol.* **136**, 1035–1046.e6.
- Park, S. J., and Im, D. S. (2019). Blockage of sphingosine-1-phosphate receptor 2 attenuates allergic asthma in mice. *Br. J. Pharmacol.* **176**, 938–949.

- Patil, M. J., Meeker, S., Bautista, D., Dong, X., and Undem, B. J. (2019). Sphingosine-1-phosphate activates mouse vagal airway afferent C-fibres via S1PR3 receptors. *J. Physiol.* **597**, 2007–2019.
- Pichavant, M., Goya, S., Meyer, E. H., Johnston, R. A., Kim, H. Y., Matangkasombut, P., Zhu, M., Iwakura, Y., Savage, P. B., Dekruyff, R. H., et al. (2008). Ozone exposure in a mouse model induces airway hyperreactivity that requires the presence of natural killer T cells and IL-17. *J. Exp. Med.* **205**, 385–393.
- Plopper, C. G., Chang, A. M., Pang, A., and Buckpit, A. R. (1991). Use of microdissected airways to define metabolism and cytotoxicity in murine bronchiolar epithelium. *Exp. Lung Res.* **17**, 197–212.
- Price, M. M., Oskeritzian, C. A., Falanga, Y. T., Harikumar, K. B., Allegood, J. C., Alvarez, S. E., Conrad, D., Ryan, J. J., Milstien, S., and Spiegel, S. (2013). A specific sphingosine kinase 1 inhibitor attenuates airway hyperresponsiveness and inflammation in a mast cell-dependent murine model of allergic asthma. *J. Allergy Clin. Immunol.* **131**, 501–511.e1.
- Rosenquist, N. A., Metcalf, W. J., Ryu, S. Y., Rutledge, A., Coppes, M. J., Grzymalski, J. J., Strickland, M. J., and Darrow, L. A. (2020). Acute associations between PM2.5 and ozone concentrations and asthma exacerbations among patients with and without allergic comorbidities. *J. Expo. Sci. Environ. Epidemiol.* **30**, 795–804.
- Smith, E. L., and Schuchman, E. H. (2008). The unexpected role of acid sphingomyelinase in cell death and the pathophysiology of common diseases. *FASEB J.* **22**, 3419–3431.
- Sopel, N., Kölle, J., Dumendiak, S., Koch, S., Reichel, M., Rhein, C., Kornhuber, J., and Finotto, S. (2019). Immunoregulatory role of acid sphingomyelinase in allergic asthma. *Immunology* **156**, 373–383.
- Sprong, H., Kruithof, B., Leijendekker, R., Slot, J. W., Van Meer, G., and Van Der Sluijs, P. (1998). UDP-galactose: ceramide galactosyltransferase is a class I integral membrane protein of the endoplasmic reticulum. *J. Biol. Chem.* **273**, 25880–25888.
- Stevens, N. C., Edwards, P. C., Tran, L. M., Ding, X., Van Winkle, L. S., and Fiehn, O. (2021). Metabolomics of lung microdissections reveals region- and sex-specific metabolic effects of acute naphthalene exposure in mice. *Toxicol. Sci.* **184**, 214–222.
- Tsugawa, H., Cajka, T., Kind, T., Ma, Y., Higgins, B., Ikeda, K., Kanazawa, M., Vanderghenst, J., Fiehn, O., and Arita, M. (2015). MS-dial: data-independent MS/MS deconvolution for comprehensive metabolome analysis. *Nat. Methods.* **12**, 523–526.
- Tetreault, L. F., Doucet, M., Gamache, P., Fournier, M., Brand, A., Kosatsky, T., and Smargiassi, A. (2016). Severe and moderate asthma exacerbations in asthmatic children and exposure to ambient air pollutants. *IJERPH* **13**, 771.
- Uhlson, C., Harrison, K., Allen, C. B., Ahmad, S., White, C. W., and Murphy, R. C. (2002). Oxidized phospholipids derived from ozone-treated lung surfactant extract reduce macrophage and epithelial cell viability. *Chem. Res. Toxicol.* **15**, 896–906.
- Williams, A. S., Issa, R., Durham, A., Leung, S. Y., Kapoun, A., Medicherla, S., Higgins, L. S., Adcock, I. M., and Chung, K. F. (2008). Role of p38 mitogen-activated protein kinase in ozone-induced airway hyperresponsiveness and inflammation. *Eur. J. Pharmacol.* **600**, 117–122.
- Wright, S. M., Hockey, P. M., Enhorning, G., Strong, P., Reid, K. B. M., Holgate, S. T., Djukanovic, R., and Postle, A. D. (2000). Altered airway surfactant phospholipid composition and reduced lung function in asthma. *J. Appl. Physiol.* **89**, 1283–1292.
- Yaeger, M. J., Reece, S. W., Kilburg-Basnyat, B., Hodge, M. X., Pal, A., Dunigan-Russell, K., Luo, B., You, D. J., Bonner, J. C., Spangenburg, E. E., et al. (2021). Sex differences in pulmonary eicosanoids and specialized pro-resolving mediators in response to ozone exposure. *Toxicol. Sci.* **183**, 170–183.
- Yang, Y., and Uhlig, S. (2011). The role of sphingolipids in respiratory disease. *Ther. Adv. Respir. Dis.* **5**, 325–344.
- Zehethofer, N., Bermbach, S., Hagner, S., Garn, H., Müller, J., Goldmann, T., Lindner, B., Schwudke, D., and König, P. (2015). Lipid analysis of airway epithelial cells for studying respiratory diseases. *Chromatographia* **78**, 403–413.
- Zeidan, Y. H., Wu, B. X., Jenkins, R. W., Obeid, L. M., and Hannun, Y. A. (2008). A novel role for protein kinase cδ-mediated phosphorylation of acid sphingomyelinase in UV light-induced mitochondrial injury. *FASEB J.* **22**, 183–193.
- Zhang, Y., Li, X., He, M., Zhang, G., Bao, W., Fei, X., Zhang, X., Zhang, M., and Zhang, P. (2019a). The effects of neutralizing anti-murine interleukin-17a monoclonal antibody on ozone-induced inflammation and glucocorticoids insensitivity in a murine model of asthma. *Biomed. Pharmacother.* **114**, 108786.
- Zhang, Y., Willis-Owen, S. A. G., Spiegel, S., Lloyd, C. M., Moffatt, M. F., and Cookson, W. O. C. M. (2019b). The ORMDL3 asthma gene regulates icam1 and has multiple effects on cellular inflammation. *Am. J. Respir. Crit. Care Med.* **199**, 478–488.